LANGMUIR

Article

pubs.acs.org/Langmuir

Unique Combination of Surface Energy and Lewis Acid−Base Characteristics of Superhydrophobic Cellulose Fibers

J. A. F. Gamelas,*[,†] A. Salvador,[‡] J. Hidalgo,[‡] P. J. Ferreira,[†] and A. Tejado*[,‡]

[†]Department of Chemical Engineering, CIEPQPF, University of Coimbra, Pólo II. R. Sílvio Lima, PT-3030-790 Coimbra, Portugal

[‡]Sustainable Construction Division, TECNALIA, Área Anardi 5, 20730 Azpeitia, Spain

Supporting Information

ABSTRACT: Cellulose fibers were first functionalized on their surface by silanization with trichloromethylsilane in an optimized gas−solid reaction, and the occurrence of the reaction was assessed using attenuated total reflection Fourier transform infrared (ATR-FTIR) spectroscopy. Then, the changes in the physicochemical surface properties of the material were thoroughly assessed using inverse gas chromatography (IGC) and X-ray photoelectron spectroscopy as surface specific tools. A very surprising combination of results was obtained: (i) the dispersive component of the surface energy was found to decrease from 42 to 14 mJ m^{-2} (at 40 °C), the latter figure representing one of the lowest values ever reported (by IGC) for cellulose-based materials, and (ii) both Lewis acidic and Lewis basic characters of the fiber surface, as measured by the injection into the IGC columns of 15 different vapor probes, significantly increased with silanization. Moreover, those remarkable changes in the surface properties of the material were obtained at a low degree of silanization (as shown by ATR-FTIR). The present results may have a great impact in what concerns the application of the described type of superhydrophobic cellulose fibers for the production of new biocomposites: an unusual enhanced compatibility both with low-surface-energy polymeric matrices, such as polyolefins, as well as with other types of matrices through Lewis acid−base interactions, can be predicted.

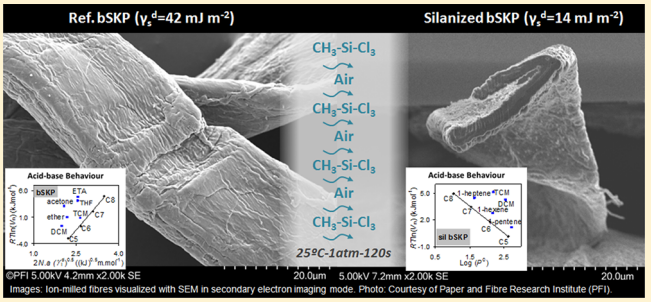

INTRODUCTION

Recent decades have witnessed a growing interest in plant-based composite materials.[1] Cellulose, either as wood particles or as cellulose pulp fibers, is being increasingly used as reinforcement for polymeric matrices, showing some interesting advantages (sustainable, flexible, nonabrasive, and so forth) over synthetic alternatives such as glass fibers. However, in these plant-based composites, obtaining good compatibility between the cellulosic fibers (markedly hydrophilic) and some of the most used polymeric matrices such as polypropylene and polyethylene (highly hydrophobic) is a major challenge that remains to be solved. Such different polarities of the two phases lead to a weak interfacial adhesion, fiber aggregation, and, as a result, low-performance composites. To obtain good mechanical properties of the composite, extensive wetting of the fibers by the polymer matrix is mandatory and thus full-surface modification of cellulose through hydrophobization treatments is a long-sought strategy.

The hydrophobization of cellulose substrates has been performed for many decades in the frame of the paper-making industry. With the general approach of deactivating the hydroxyl (OH) groups that confer cellulose with its hydrophilicity through a chemical reaction, different hydrophobizing agents such as alkyl ketene dimer, alkenyl succinic anhydride, or rosin products have been largely used to increase the water resistance of paper.[2] More recently, alternative compounds such as triglycerides,[3] acid chlorides,[4,5] different types of alkyl-terminated[6−9] and fluorine-terminated[8,10] silane derivatives, and other complex species such as glycidyl methacrylate[11] have been tested successfully at laboratory scale. Some of those compounds are so efficient that they are able to decrease the surface energy of the cellulose to a level wherein a drop of water slides off at tilt angles as low as a few degrees. This new performing limit, known as "superhydrophobicity", is also characterized by water drops forming contact angles larger than 150° with the cellulosic surface. In parallel, new methods of application have also been targeted including diverse techniques such as spray-coating,[12] dip-coating,[7,9] chemical vapor deposition (CVD),[8,13−16] plasma treatments,[10] atom transfer radical polymerizations,[11] or even designing specific processes, such as that named chromatogenic method.[4]

Among all of those methods and reactants, CVD of trichloromethylsilane (TCMS) has shown special relevance. TCMS can react not only with OH groups on the surface of the fiber to give ether bridges through a condensation reaction but also with itself, leading to the formation of a polymethylsilsesquioxane coating.[7,15] Previously, the Cl atoms are substituted by OH (thus the silane is converted into a silanol) by reaction with tiny amounts of water existing either in the air or on the

Received: November 2, 2016
Published: December 29, 2016

DOI: 10.1021/acs.langmuir.6b03970
Langmuir XXXX, XXX, XXX−XXX

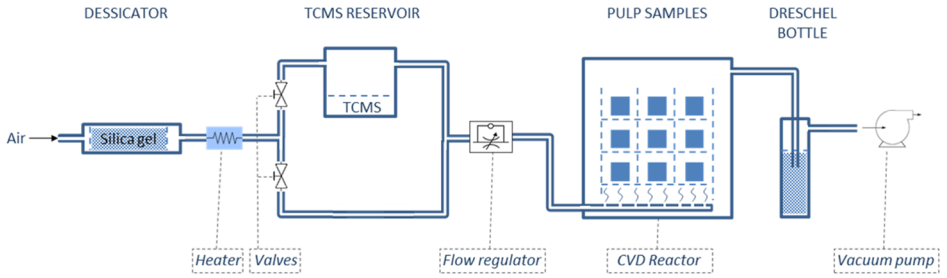

Figure 1. Diagram illustrating the CVD process for TCMS treatment.

surface of the fiber. Some of those silanol groups may remain unreacted at the end of the treatment. The hydrophobization of cellulose fibers is ultimately due to two separate effects: first, hygroscopic OH groups previously present all over the cellulose fiber are no longer available, and second, the fiber surface is coated with a Si−O−Si network decorated with CH_3 chain ends.

The high efficiency of this silanization treatment, which can result in individualized superhydrophobic cellulose fibers,[16,17] shows great potential to many diverse applications, such as in the production of reinforcing agents for a new series of biocomposites based on apolar matrices. The thorough characterization of the surface properties of the new silanated cellulose fibers reported in this work is meant to provide valuable information to anticipate their behavior.[18]

Inverse gas chromatography (IGC) presents as a highly sensitive and versatile physicochemical characterization technique to properly assess the surface of fibrous materials.[19−21] By measuring the retention times of different vapor probes on the surface of the solid material under analysis (stationary phase) and by using known calculation approaches, a wide range of physicochemical surface parameters can be obtained for the material, assessing some of which by other techniques is not possible. In particular, this technique is advantageous over the classical contact-angle measurements for the correct analysis of porous, rough, and heterogeneous surfaces. IGC has been already used in the past to study the changes in the surface properties of cellulose and lignocellulosic materials occurring during functionalization reactions.[20,21] The reactions studied include esterification by acyl chlorides,[22] fatty acids,[23] or anhydrides;[24] coupling reactions with reagents containing isocyanate moieties;[24,25] chemical modification with dichlorodiethylsilane or γ-aminopropyltriethoxysilane;[26−28] and TEMPO-mediated oxidation,[29] among others.

In this work, IGC has been used for the thorough surface physicochemical characterization of bleached softwood kraft pulp (bSKP) fibers before and after being subjected to the aforementioned CVD treatment with TCMS. The properties such as the dispersive component of the surface energy, specific components of the probe's free energy of adsorption, Lewis acid−base character of the surface, and surface nanoroughness parameter have been elucidated using a wide range of IGC probes (with different polarities, sizes, and Lewis acid−base characters) and models. Attenuated total reflectance Fourier transform infrared (ATR-FTIR) spectroscopy and X-ray photoelectron spectroscopy (XPS) were also used to obtain information on the chemical structure of the material surface and to complement the results obtained by IGC. The results are presented and critically discussed.

EXPERIMENTAL SECTION

Materials. bSKP, provided by local paper mill as never-dried pulp at 21% consistency, was used in this study. Before being used, the pulp was further purified three times with 0.5 wt % of $NaClO_2$ (relative to a dry pulp) in acetate buffer at pH 4.8, allowing the mixture to react for 1 h at 70 °C followed by filtering and washing with distilled water. The lignin content was found to be <0.1 wt % (TAPPI T222 om-02 method), and the ash content was 0.3 wt % (TAPPI T211 om-12). Cellulose and hemicelluloses accounted for, respectively, 84.6 and 12.5 wt %, both determined using the Rowell method (more information is provided in the Supporting Information section). The carboxyl group content of the pulp was determined through conductometric titration and found to be 0.046 mmol per gram of pulp after averaging three measurements. Ethanol (absolute, 99.8% purity) and TCMS (99.0% purity) were obtained from Sigma and used without further purification. All probes for the IGC analysis were of chromatographic grade and were used as received from Sigma-Aldrich.

Cellulose Hydrophobization via CVD. Pulp hydrophobization was carried out based on a previous work,[16] but the development of a new semicontinuous protocol is schematized in Figure 1. The new setup allows better control over the TCMS dosage, which can be modulated by varying the concentration in air through a valve system, by adding a post-treatment cleaning stage, by blowing air throughout the samples, and by working under security conditions. If needed, the new setup also permits monitoring the reaction rate by recording the pH of the solution contained at the Dreschel bottle, which otherwise neutralizes the exit stream coming from the reactor. The resulting weight increase in the cellulose fibers after the CVD treatment with TCMS was 1.2 wt % under the conditions used in this work. More details are provided in the Supporting Information.

ATR-FTIR. ATR-FTIR was used to confirm the success of the silanization reaction after oven-drying at 60 °C for 2 h TCMS-treated (and nontreated) pulp fibers. The FTIR measurements were recorded using a Bruker Tensor 27 spectrometer equipped with a MKII Golden Gate ATR accessory. The spectra were recorded in the 600−1700 cm^{-1} range with a resolution of 4 cm^{-1} and a number of scans of 256. The background spectra were recorded before every sampling.

X-ray Photoelectron Spectroscopy. The X-ray photoelectron spectra were recorded using Kratos AXIS Ultra HAS equipment. The analysis was carried out with a monochromatic Al Kα X-ray source (1486.7 eV), operating at 15 kV (90 W), in the fixed analyzer transmission mode, with a pass energy of 80 eV. Wide-scan survey spectra were recorded at take-off angle of 90° and between 0 and 1350 eV binding energy with a step size of 1 eV and a dwell time of 200 ms. High-resolution C 1s and Si 2p spectra were obtained with a step size of 0.1 eV and a dwell time of 1500 ms; O 1s spectra were obtained with a step size of 0.1 eV and a dwell time of 600 ms. The peak-fitting of the high-resolution spectra was performed using Gaussian−Lorentzian peak shapes and Shirley-type background subtraction. Pellets of 1 mm thickness were previously prepared for the analysis by pressing the samples at approximately 40 MPa for 2 min.

Inverse Gas Chromatography Analysis. The IGC analysis was performed using a DANI GC 1000 digital pressure control gas chromatograph equipped with a hydrogen flame ionization detector. Stainless steel columns (0.5 m long and 0.4 cm inside diameter) were washed with acetone and dried before packing. For each analysis, 1.5−

DOI: 10.1021/acs.langmuir.6b03970
Langmuir XXXX, XXX, XXX−XXX

2 g of fibers was packed into the gas chromatograph column, before which the samples were gently milled using a coffee mill with blunt blades to avoid the presence of large agglomerates of the fibers. The packed columns were shaped in a smooth "U" to fit the detector/injector geometry of the instrument and then conditioned overnight at 105 °C, under a helium flow, before any measurements were recorded. The measurements were recorded at the column temperatures of 40–55 °C (with intervals of 5 °C) using the injector and detector kept at 180 and 200 °C, respectively. Helium was used as a carrier gas with a constant flow rate of 6–7 mL/min. Small quantities of vapor probes (<1 μL) were injected into the carrier gas, allowing work to be performed under infinite dilution conditions. The probes used for the IGC data collection were *n*-pentane (C5), *n*-hexane (C6), *n*-heptane (C7), *n*-octane (C8), *n*-nonane (C9), trichloromethane (TCM, Lewis acidic probe), dichloromethane (DCM, acidic), tetrahydrofurane (THF, basic), ethyl ether (basic), ethyl acetate (ETA, amphoteric), acetone (amphoteric), 1-pentene, 1-hexene, and 1-heptene (weak Lewis bases), and cyclohexane. Methane was used as the reference probe. The retention times were the average of three injections and were determined using the Conder and Young method (Figure S1).[30] Note that for less symmetrical chromatograms, the Conder and Young method provides a more reliable determination of the peak mass center than the peak maximum. In some cases, and for a matter of comparison, the determination of the retention time at the peak maximum was also considered. Obviously, for perfectly symmetric chromatograms, the results obtained by the two methods coincide. The coefficient of variation in the retention time measurements was always lower than 6%.

IGC Theory. The theoretical aspects of IGC with relevance to the present work are summarized in the Supporting Information section.[19,21,31,32] From the retention time data, the dispersive component of the surface free energy of each material (γ_s^d), the specific component of the free energy of adsorption (ΔG_a^s) of different Lewis acid–base probes on the surface of materials (obtained using several calculation approaches), and a nanomorphology index (IMχ_T) have been obtained.

RESULTS AND DISCUSSION

Modification of the Cellulose Fibers Assessed by ATR-FTIR. The success of the hydrophobization treatment was assessed through ATR-FTIR measurements, by monitoring the appearance of new peaks at 1275 and 780 cm^{-1} (Figure 2), which correspond respectively to the symmetric bending vibration of CH_3 groups attached to Si atoms and to the stretching vibration of Si–C bonds as reported earlier.[14,15] The intensity increase in these bands was quite subtle for the bSKP-treated sample, suggesting that the degree of modification was low. However, at a thin outer surface layer of the sample, the extent of silanization was significant, as will be shown below by XPS (in the following subsection). The absorption bands of the Si–O–Si bonds created during the silanization treatment remain invisible as they overlap with the characteristic cellulose C–O stretching bands present in the 1160–1000 cm^{-1} range.

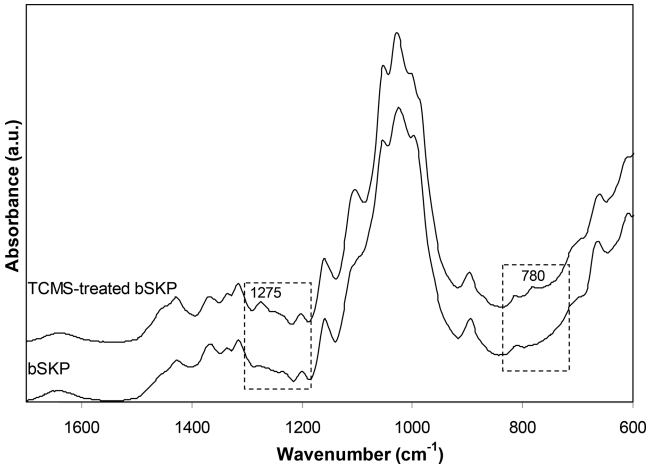

Figure 2. ATR-FTIR spectra of the untreated and TCMS-treated bSKP (with highlighted regions).

Surface Chemical Composition of the Silanized Fibers Assessed by X-ray Photoelectron Spectroscopy. To check for the success of the surface silanization process, the original and functionalized fibers were analyzed by XPS, which, similar to IGC, is a surface specific technique (up to approximately 10 nm depth). The most relevant XPS results are summarized in Table 1. As expected, C and O were found as major elements and also Si was found on the surface of the silanized fibers. After silanization, the atomic percentage of carbon decreased significantly from 63 to 40%, whereas silicon contributed to 19% of all elements (excluding hydrogen that is not counted by the XPS analysis). The Si/C atomic ratio was 0.48 for the silanized bSKP, confirming the modification of the fiber surface by the employed gas–solid silanization method. Accordingly, the O/C atomic ratio was also higher for the silanized pulp. The peak-fitting of the high-resolution C 1s spectra of the different materials showed four main components, with those corresponding to aliphatic carbon (C1: C–C, C–H) and carbon in C–O bonds (C2) as the dominant ones (Figure 3A,B and Table 1). After modification, the increase in the C1 component (in normalized values) accompanied by the concomitant decrease in the other components is an indication of the introduction of methyl groups in the cellulose chain. Following silanization, one signal was observed in the high-resolution Si 2p spectrum (Figure 3C). Another interesting result of the XPS analysis was that no chlorine has been detected (Cl 2p and Cl 2s signals) on the material surface, showing that the eventual contamination of the final product by the reagent used in the synthesis (TCMS) or by the chloric acid produced during the reaction was negligible. This also indicates that the washing procedure was good enough to remove any contaminants. A subsequent analysis was also carried out by energy-dispersive X-ray spectroscopy, and no chlorine was detected either. Thus, from the results of FTIR and XPS spectroscopy, it can be concluded that the modification of the cellulosic material occurred.

Dispersive Components of the Surface Free Energy. The dispersive component of the surface energy (at different temperatures) of the bSKP before and after its treatment with TCMS was determined, following the Schultz and Lavielle approach.[34] The results are plotted in Figure 4. The bSKP presented a γ_s^d value (at 40 °C) of 42.3 mJ m^{-2}, which, after silanization, decreased to almost one-third (to 14.5 mJ m^{-2}). These results clearly indicate the hydrophobization of the cellulose fiber surface and may be closely related to the introduction of methyl groups into the cellulose chains. These small apolar groups not only have poor ability to establish strong London/Debye interactions but also, being more exposed on the material surface, limit the interaction of cellulose OH groups and apolar entities with the apolar probes (*n*-alkanes).

Other distinct features were detected when comparing the influence of temperatures on the γ_s^d value of materials, whereas for unfunctionalized bSKP, γ_s^d decreases with temperature, at least within the studied region, that is, between 40 and 55 °C

DOI: 10.1021/acs.langmuir.6b03970
Langmuir XXXX, XXX, XXX–XXX

Table 1. XPS Atomic Percentages and Results of the Peak Fitting of C 1s Signal for bSKP and Silanized bSKP

	elements (%)			atomic ratios		C 1s components (%)[a]			
material	C	O	Si	O/C	Si/C	C1	C2	C3	C4
bSKP	62.9	37.1		0.59		22.4	60.6	14.9	2.1
Sil bSKP	39.5	41.5	19.0	1.05	0.48	65.8	27.0	6.5	0.7

[a]C 1s components are normalized to 100%. C1 corresponds to carbon that is linked only to hydrogen or to carbon (−C−H; −C−C, C═C), C2 corresponds to carbon that is linked to a single oxygen (−C−O), C3 is due to O−C−O or −C═O bonds, and C4 is due to −COO bonds.[33]

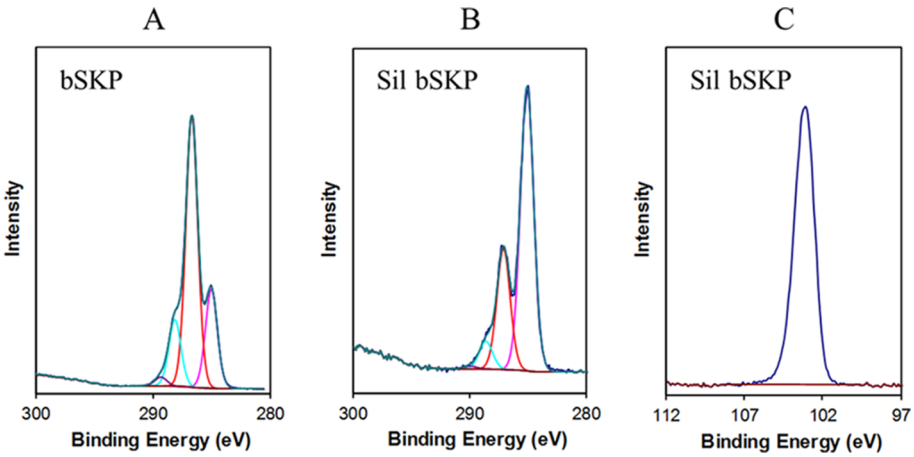

Figure 3. High-resolution XP spectra with peak-fitting in the region of carbon-binding energies for bSKP (A) and silanized bSKP (B) and high-resolution XP spectrum in the region of silicon-binding energies for silanized bSKP (C).

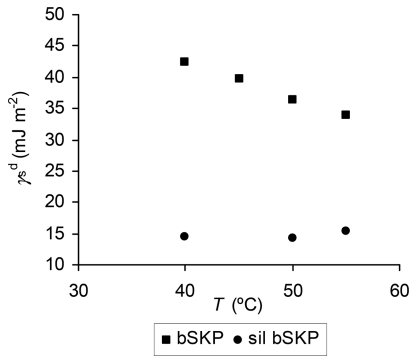

Figure 4. γ_s^d values at several temperatures for bSKP and silanized bSKP.

(Figure 4), being $-d\gamma_s^d/dT$ of 0.58 mJ m^{-2} K^{-1} for this material; for the silanized cellulose, on the other hand, γ_s^d was found to be reasonably constant in the range of studied temperatures (Figure 4). The decrease in γ_s^d with temperature is a normal behavior for cellulosic fibers[29,35] and other materials and indicates the effect of an entropic contribution for the reduction in the surface energy. In the case of silanized cellulose, it seems that the surface energy or at least its dispersive component is not significantly affected by the variation in temperature, that is, a probable very small variation in γ_s^d with temperature, not clearly detected by IGC, occurs.

Additionally, and to our knowledge, the present γ_s^d values are also among the lowest ones reported so far for modified cellulosic materials.[21] For instance, the modification of cellulose by esterification with palmitoyl chloride decreases the γ_s^d value from 44 to 28 mJ m^{-2} (at 70 °C),[22] whereas cellulose acetate butyrate and hydroxyethylcellulose present a dispersive component of the surface energy of 18 mJ m^{-2} at 50 °C.[36,37] On the other hand, it was reported that the surface modification of quartz silica particles with methyltrimethoxysilane in water (with the formation of a siloxane coating) produced, as well, an impressive reduction in γ_s^d from the original 255 to 36 mJ m^{-2} for a full surface coverage by the silane (the initial value is quite different from that of cellulose but the decrease was, similarly, very significant).[38] When several alkyltrichlorosilanes have been applied to other OH-containing substrates, such as glass slides or silicon wafers, the treatment also resulted in both cases in the reduction of γ_s^d (as determined from the contact-angle measurements).[39] This allows it to be concluded that the methyl groups are indeed responsible for the high decrease in the dispersive component of the surface energy that occurred during the cellulose modification.

We have also conducted similar silanization reactions on a thermomechanical cellulosic pulp, that is, less pure cellulose containing a considerable amount of lignin (25.8% according to TAPPI T222 om-02). After modification with TCMS using the same CVD technique, surface properties similar to those reported here for the bleached cellulosic pulp have been obtained, including similar values for the dispersive component of the surface energy (14−15 mJ m^{-2}). This shows that the purity of the substrate is not crucial and suggests that the physicochemical properties of the surface of the silanized cellulosic fibers should be closer to those of a methyl−silica coating. These results will be published in a forthcoming paper.

Lewis Acid−Base Character. The next step consisted of the evaluation of the acid−base properties of the new materials. For this, a wide range of Lewis acidic, basic, and amphoteric probes was injected into the IGC column and the corresponding specific interaction parameters with the material surface were determined using different approaches. The main results, obtained using the Schultz and Lavielle[34] (Figure 5) and Dorris and Gray[40] (Figure 6) approaches, expressed in terms of ΔG_a^s of each probe are summarized in Table 2.

DOI: 10.1021/acs.langmuir.6b03970
Langmuir XXXX, XXX, XXX−XXX

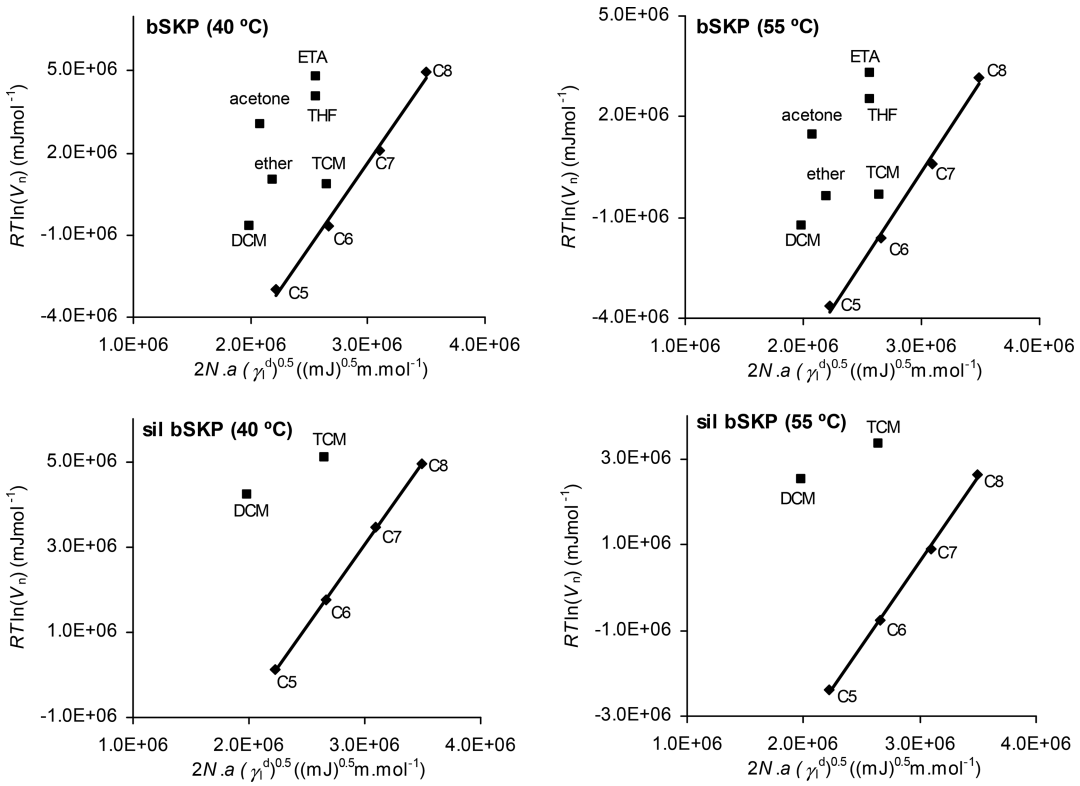

Figure 5. Plots of $RT\ln(V_n)$ vs $2N{\cdot}a(\gamma_1^d)^{0.5}$ for the adsorption of *n*-alkanes and Lewis acid−base probes on bSKP and silanized bSKP (at 40 and 55 °C).

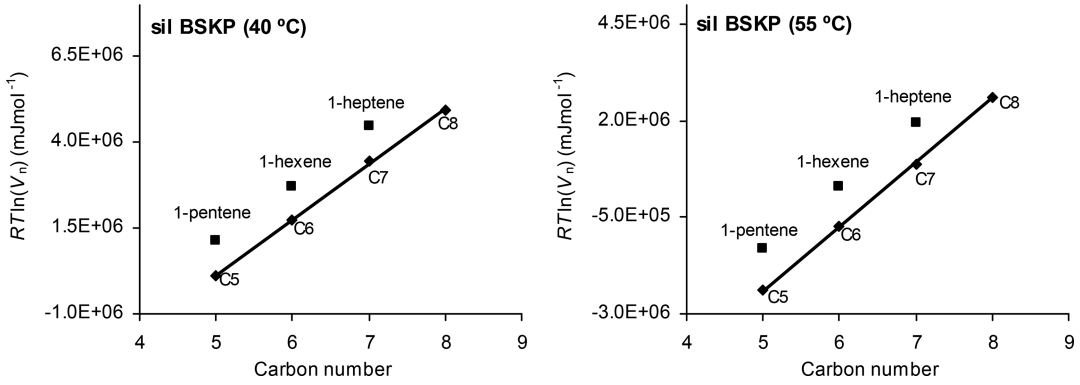

Figure 6. Plots of $RT\ln(V_n)$ vs number of carbon atoms for the adsorption of *n*-alkanes and 1-alkenes on silanized bSKP (at 40 and 55 °C).

Table 2. Specific Component of the Free Energy of Adsorption ($-\Delta G_a^s$, kJ mol^{-1}) of Lewis Acid−Base Probes on the Surface of bSKP and Silanized bSKP

samples	probes						
	acidic[a]		basic[a]		amphoteric[a]		
untreated	TCM	DCM	THF	ether	ETA	acetone	ΔG_a^s (THF)/ΔG_a^s (TCM)
bSKP (40 °C)	1.56	4.37	5.33	4.70	6.12	7.49	3.4
bSKP (55 °C)	1.45	4.43	4.81	4.09	5.63	6.54	3.3
samples	probes						
	acidic[a]		weak basic probes[b]				
TCMS-treated	TCM	DCM	1-pentene	1-hexene	1-heptene		
Sil bSKP (40 °C)	3.37	5.02	1.01	0.98	1.01		
Sil bSKP (55 °C)	4.11	5.90	1.09	1.06	1.07		

[a]Determined using the Schultz and Lavielle approach. [b]Determined using the Dorris and Gray approach.

DOI: 10.1021/acs.langmuir.6b03970
Langmuir XXXX, XXX, XXX−XXX

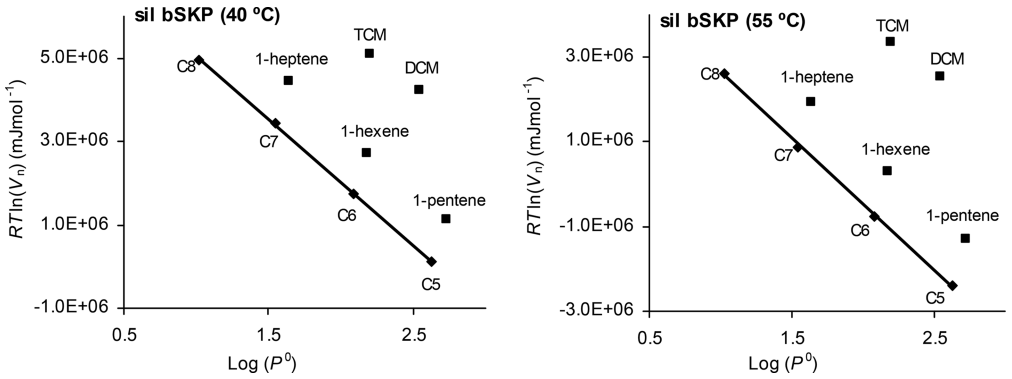

Figure 7. Plots of $RT\ln(V_n)$ vs saturated vapor pressure (p^0) of the different probes for silanized bSKP (at 40 and 55 °C).

For the bSKP, the affinity with Lewis basic and Lewis amphoteric probes was higher than that with the Lewis acidic probe of similar molecular surface area, and the ratios $-\Delta G_a^s$ (THF)/$-\Delta G_a^s$ (TCM) and $-\Delta G_a^s$ (ether)/$-\Delta G_a^s$ (TCM) were 3.4 (Table 2) and 3.0, respectively. Note that for DCM a significantly higher specific interaction (approximately 3 times) than that of TCM was found. This can be attributed mainly to the much lower molecular surface area of DCM (Table S1) that enables higher specific interactions owing to the less steric restriction. Besides, DCM has a lower Lewis acidity than TCM (although both have a donor number of zero) (Table S1), and for a dominant acidic surface, a higher specific interaction with DCM is thus to be expected. These results, in agreement with those already reported for the bleached kraft pulps,[35,41] indicate a prevalence of Lewis acidity over Lewis basicity of bSKP. This, as already reported, is supposed to be due mainly to the influence of the presence of a large amount of accessible acidic OH groups on the cellulose surface.

With the modification, the changes in the acid−base properties were striking. It was noted that the typical Lewis basic probes such as THF and ethyl ether or the amphoteric ones (acetone and ETA) were retained too strongly in the material that impeded the measurement of their specific interaction with the functionalized material. This was considered to be an evidence of a high Lewis acidic character of the silanized bSKP surface. At the same time, the specific interaction parameter with Lewis acidic probes increased significantly for both TCM and DCM but more pronounced for TCM, that is, about 2.5 times (Table 2). Thus, the overall results seem to indicate that both the Lewis acidity and Lewis basicity of the cellulosic material surface were increased by silanization. Lewis acidity and basicity can follow a similar trend if simultaneously new functional acidic and basic groups are attached to the surface of the material, namely, by their grafting into the cellulose chains. In the present case, the introduction of both basic siloxane (Si−O−Si) and acidic silanol (Si−OH) groups may be responsible for the increase in the Lewis acid−base character of the surface of the fiber While the former groups will enhance the formation of Lewis acid−base adducts with mainly Lewis acidic probes, the latter groups will strengthen mainly the interactions with Lewis basic probes.

As an alternative to assess the Lewis acidic behavior of the material surface, the retention times with weak Lewis bases (1-pentene, 1-hexene, and 1-heptene) were measured, and the corresponding specific interactions with the material surface were determined based on the Dorris and Gray method (Figure 6 and Table 2). For the initial bSKP, the retention time (and retention volume) of each 1-alkene was equal to that of the corresponding *n*-alkane (i.e., no differences were detected between the chromatograms of 1-pentene and *n*-pentane, 1-hexene and *n*-hexane, or 1-heptene and *n*-heptane). The functionalized bSKP exhibited a quite different behavior, that is, the retention times of alkenes were always higher than those of the corresponding alkanes (Figure S2); therefore, a specific interaction with the π electron donor bases (vs *n*-alkanes) was detected (Figure 6). Thus, following the remarkably high interaction with the stronger Lewis basic probes (not possible to measure) mentioned above, a specific interaction was also established with weak Lewis bases. To our knowledge, this behavior was never reported before for the cellulosic materials as a result of a surface functionalization process. Even so, all values obtained for the π interactions for the silanized bSKP (around 1 kJ mol^{-1}) were still of lower magnitude than those observed, for instance, for mineral species like clays, hydroxyapatites, and calcium carbonates, among others (3−5 kJ mol^{-1}).[42−44] Similar to the dispersive component of the surface energy, a remarkable change in the acid−base character of the cellulosic surface was then able to be measured by IGC.

Following an in-depth search in the scientific literature, the closest we could find to the present results was related to the modification of quartz silica particles with methyltrimethoxysilane in water to produce a siloxane coating.[38] The authors reported that this treatment, besides highly decreasing the dispersive component of the surface energy, as aforementioned, also provided enhanced Lewis specific interactions with TCM ($-\Delta G_a^s$ (TCM) variation from 4.1 to 5.6 kJ mol^{-1}). On the other hand, they reported that the interactions with Lewis basis probes (THF) were too strong and not possible to measure (probe not desorbed from the column) for both the original and the silane-treated particles; although not quantified, this was an indication that the final material also possessed a strong Lewis basic character because if a decrease in the $-\Delta G_a^s$ (THF) was detected, the latter would be possibly measured by IGC. Overall, it can be proposed that the (neutral) methyl groups inserted in the siloxane chain, as they are relatively small, do not hinder (by steric hindrance) the access of the Lewis acid−base probes to the acidic and basic sites in the neighborhood of the silicon atoms to which they are attached. Therefore, the acid−base properties of the cellulose can even be enhanced by the coating with methyl−silica with an accompanied decrease in the dispersive component of the surface energy.

It can also be noted that the temperature increase did not significantly affect the acid−base properties of both the bSKP material (same acidity to basicity ratio at 40 and 55 °C, see the last column on Table 2) and the silanized material (interactions of weak Lewis bases at 40 and 55 °C were similar; Table 2).

DOI: 10.1021/acs.langmuir.6b03970
Langmuir XXXX, XXX, XXX−XXX

Table 3. Values of Specific Interaction Energies ($-\Delta G_a^s$, kJ mol^{-1}) Assessed by the Flour and Papirer Method for Lewis Acid–Base Probes on Silanized Cellulosic Pulp

material	temperature (°C)	TCM	DCM	1-pentene	1-hexene	1-heptene	DCM/1-pentene	TCM/1-hexene
Sil bSKP	40	3.68	3.86	1.31	1.23	1.35	3.0	3.0
	55	4.43	4.71	1.42	1.32	1.31	3.3	3.4

The interactions of the different probes with the silanized pulp surface can be compared based on the plots, as shown in Figure 7 (Saint Flour and Papirer approach). This method has the advantage over the Schultz and Lavielle and Dorris and Gray approaches that all probes can be compared on the same basis because it requires only the knowledge of the saturated vapor pressure of the measured probes (note that for the application of the Schultz and Lavielle approach, the molecular area values of all probes must be known and no reliable values are found to be held for 1-alkenes; besides, the *a* values of nonspherical adsorbed molecules may change depending on the orientation of the molecules on the material surface). The results (Table 3) confirmed in general the trends shown above for acidic probes and 1-alkenes. However, when using the Flour and Papirer calculation method, the specific interaction of TCM approaches that of DCM (Table 3), whereas by the Schultz and Lavielle method, the values obtained for these specific interactions (Table 2) differed more. This type of difference was already reported for other materials and was interpreted as being the result of the different assumptions underlying the two employed methods and of the uncertainty in the molecular area value of adsorbed DCM.[43] The ratios TCM/1-hexene and DCM/1-pentene can provide a relative measure of the specific affinities of weak Lewis bases and Lewis acidic probes of similar volatility and were also determined (Table 3). Although the silanized material is demonstrated to be more Lewis acidic than basic (strong Lewis basic probes are not easily eluted), these basicity-to-acidity ratios were always higher than 1 (between 3.0 and 3.4), showing that specific interactions with Lewis acidic probes are, even so, higher than those with 1-alkenes.

Finally, a nanomorphology index (IMχ_T) based on the measurement of retention time of a cyclic alkane probe, cyclohexane, was also determined. The main purpose of this determination was to check whether some of the variations shown above for the acid–base character of the fibers during silanization could also be due to the differences in the nanoroughness of the fiber. For the bSKP before and after silanization, it was found that the IMχ_T parameter always presents a negative value (Table 4), indicating the presence of some roughness at the molecular scale of the fibers. After functionalization, the values of IMχ_T became more negative, indicating an even rougher surface. This was more evident for the measurements made at 40 °C where the differences between the silanized material and the original bSKP were considerably greater (Table 4). It is interesting to note the influence of the method used for the measurement of the retention time, at the peak maximum or at the mass center of the peak (Conder and Young), on the value obtained for IMχ_T (Table 4). In fact, significantly different values were obtained for the silanized bSKP at 40 °C (where the chromatograms are more asymmetric, Figure S3). However, the results using the mass center values should be viewed as the more appropriate ones because, in this case, the asymmetry of the chromatogram is also being taken into account. It is widely accepted that the measurement of the retention time at the peak maximum is valid only for highly symmetric chromatograms. Nevertheless, the consistent result is an increase in the nanoroughness of the fiber after silanization. A high nanoroughness of the fiber has also been suggested previously for silanized filter paper based on the scanning electron microscopy images.[6,14]

Table 4. Morphological Index (IMχ_T) at Different Temperatures and by Using Different Methods of Retention Time Determination for bSKP and Silanized bSKP

material	temperature (°C)	peak maximum	CY method
bSKP	40	−5.6	−5.6
	55	−5.8	−5.8
Sil bSKP	40	−12.8	−16.2
	55	−8.2	−8.4

Considering that after silanization the surface of the fibers becomes rougher at the molecular/nanoscale, it is unlikely that the aforementioned increase in the specific interactions of the material surface with both Lewis acidic (particularly with TCM relative to DCM) and basic probes with modification is due to the changes in the nanoroughness of the fiber. Such an influence would necessarily require that the hydrophobized fibers would be smoother at the molecular scale than the initial raw material, thus providing higher specific interactions with the bulky probes.[42] Therefore, the variations in the acid–base character during the silanization of the fibers should be mainly attributed to the changes in the fiber's surface chemical structure.

CONCLUSIONS

The functionalization of cellulosic fibers with TCMS via CVD reaction generated a superhydrophobic material with apparently unique surface characteristics, never reported before for cellulose-based materials. Under infinite dilution conditions, IGC revealed that the resultant silanized fibers have one of the lowest values of the dispersive component of the surface energy reported so far for modified cellulosic fibers (approximately 14 mJ m^{-2}). In combination with this and based on the measurement of the specific interactions of a wide range of Lewis acid–base probes, the simultaneous enhancement in both Lewis acidic and Lewis basic character of the fibers was also found. In particular, a specific π interaction with 1-alkenes was observed for the silanized material, whereas this specific interaction was zero for the reference cellulosic pulp. These results were tentatively ascribed to the incorporation of silanol (mainly acidic) and siloxane (mainly basic) moieties on the cellulose chains, whereas the introduction of terminal methyl groups would be responsible for the low value obtained for the dispersive component of the surface energy.

The findings of the present work, namely, the coexistence in the same material of a very low surface energy (dispersive component) and a high Lewis acid–base character, besides being completely novel, may have high relevance in the production of new biocomposites. In fact, while the low dispersive component of the surface energy may increase the compatibility of the new functionalized cellulosic material with

DOI: 10.1021/acs.langmuir.6b03970
Langmuir XXXX, XXX, XXX–XXX

hydrophobic polymeric matrices, its acid−base character may provide compatibility with other different type of matrices that are able to establish Lewis acid−base interactions with the cellulosic filler.

■ ASSOCIATED CONTENT

Supporting Information

The Supporting Information is available free of charge on the ACS Publications website at DOI: 10.1021/acs.langmuir.6b03970.

Additional information to complement the Introduction and Experimental Section, including the aspects of IGC theory; chromatograms illustrating some of the phenomena described in the article (PDF)

■ AUTHOR INFORMATION

Corresponding Authors

*E-mail: jafgas@eq.uc.pt (J.A.F.G.). Tel.: 00351239798740.
*E-mail: alvaro.tejado@tecnalia.com (A.T.). Tel.: 0034943105300.

Notes

The authors declare no competing financial interest.

■ ACKNOWLEDGMENTS

The authors acknowledge Gary Chinga-Carrasco and the Paper and Fibre Research Institute (PFI) for the acquisition of the SEM images and the COST Action FP1105 for funding a Short Term Scientific Mission in the framework of which part of the work was developed.

■ REFERENCES

(1) Kalia, S.; Dufresne, A.; Cherian, B. M.; Kaith, B. S.; Avérous, L.; Njuguna, J.; Nassiopoulos, E. Cellulose-Based Bio- and Nanocomposites: A Review. *Int. J. Polym. Sci.* **2011**, *2011*, 837875.

(2) Hubbe, M. A. Paper's Resistance to Wetting—A Review of Internal Sizing Chemicals and Their Effects. *BioResources* **2006**, *2*, 106−145.

(3) Dankovich, T. A.; Hsieh, Y.-L. Surface Modification of Cellulose with Plant Triglycerides for Hydrophobicity. *Cellulose* **2007**, *14*, 469−480.

(4) Berlioz, S.; Stinga, C.; Condoret, J.; Samain, D. SFGP 2007-Investigation of a Novel Principle of Chemical Grafting for Modification of Cellulose Fibers. *Int. J. Chem. React. Eng.* **2008**, *6*, A2.

(5) Schmid, M.; Benz, A.; Stinga, C.; Samain, D.; Zeyer, K. P. Fundamental Investigations Regarding Barrier Properties of Grafted PVOH Layers. *Int. J. Polym. Sci.* **2012**, *2012*, 637837.

(6) Cunha, A. G.; Gandini, A. Turning Polysaccharides Into Hydrophobic Materials: A Critical Review. Part 1 Cellulose. *Cellulose* **2010**, *17*, 875−889.

(7) Li, S.; Zhang, S.; Wang, X. Fabrication of Superhydrophobic Cellulose-Based Materials through a Solution-Immersion Process. *Langmuir* **2008**, *24*, 5585−5590.

(8) Oh, M.-J.; Lee, S.-Y.; Paik, K.-H. Preparation of Hydrophobic Self-Assembled Monolayers on Paper Surface with Silanes. *J. Ind. Eng. Chem.* **2011**, *17*, 149−153.

(9) Tang, Z.; Li, H.; Hess, D. W.; Breedveld, V. Effect of Chain Length on the Wetting Properties of Alkyltrichlorosilane Coated Cellulose-Based Paper. *Cellulose* **2016**, *23*, 1401−1413.

(10) Navarro, F.; Dávalos, F.; Denes, F.; Cruz, L. E.; Young, R. A.; Ramos, J. Highly Hydrophobic Sisal Chemithermomechanical Pulp (CTMP) Paper by Fluorotrimethylsilane Plasma Treatment. *Cellulose* **2003**, *10*, 411−424.

(11) Nyström, D.; Lindqvist, J.; Östmark, E.; Antoni, P.; Carlmark, A.; Hult, A.; Malmström, E. Superhydrophobic and Self-Cleaning Bio-Fiber Surfaces via ATRP and Subsequent Postfunctionalization. *ACS Appl. Mater. Interfaces* **2009**, *1*, 816−823.

(12) Ogihara, H.; Xie, J.; Okagaki, J.; Saji, T. Simple Method for Preparing Superhydrophobic Paper: Spray-Deposited Hydrophobic Silica Nanoparticle Coatings Exhibit High Water-Repellency and Transparency. *Langmuir* **2012**, *28*, 4605−4608.

(13) Zhang, H.; Kannangara, D.; Hilder, M.; Ettl, R.; Shen, W. The Role of Vapour Deposition in the Hydrophobization Treatment of Cellulose Fibres Using Alkyl Ketene Dimers and Alkenyl Succinic Acid Anhydrides. *Colloids Surf., A* **2007**, *297*, 203−210.

(14) Cunha, A. G.; Freire, C.; Silvestre, A.; Neto, C. P.; Gandini, A.; Belgacem, M. N.; Chaussy, D.; Beneventi, D. Preparation of Highly Hydrophobic and Lipophobic Cellulose Fibers by a Straightforward Gas−Solid Reaction. *J. Colloid Interface Sci.* **2010**, *344*, 588−595.

(15) Li, S.; Xie, H.; Zhang, S.; Wang, X. Facile Transformation of Hydrophilic Cellulose into Superhydrophobic Cellulose. *Chem. Commun.* **2007**, 4857−4859.

(16) Tejado, A.; Alam, M. N.; Chen, W. C.; van de Ven, T. G. M. Superhydrophobic Foam-Like Cellulose Made of Hydrophobized Cellulose Fibres. *Cellulose* **2014**, *21*, 1735−1743.

(17) Chen, W. C.; Tejado, A.; Alam, M. N.; van de Ven, T. G. M. Hydrophobic Cellulose: A Material that Expands Upon Drying. *Cellulose* **2015**, *22*, 2749−2754.

(18) Gardner, D. J.; Oporto, G. S.; Mills, R.; Samir, M. A. S. A. Adhesion and surface issues in cellulose and nanocellulose. *J. Adhes. Sci. Technol.* **2008**, *22*, 545−567.

(19) Mukhopadhyay, P.; Schreiber, H. P. Aspects of Acid−Base Interactions and Use of Inverse Gas Chromatography. *Colloids Surf., A* **1995**, *100*, 47−71.

(20) Belgacem, M. N. Characterization of Polysaccharides, Lignin and Other Woody Components by Inverse Gas Chromatography: A Review. *Cellul. Chem. Technol.* **2000**, *34*, 357−383.

(21) Gamelas, J. A. F. The Surface Properties of Cellulose and Lignocellulosic Materials Assessed by Inverse Gas Chromatography: A Review. *Cellulose* **2013**, *20*, 2675−2693.

(22) Gauthier, H.; Coupas, A.-C.; Villemagne, P.; Gauthier, R. Physicochemical Modifications of Partially Esterified Cellulose Evidenced by Inverse Gas Chromatography. *J. Appl. Polym. Sci.* **1998**, *69*, 2195−2203.

(23) Jandura, P.; Riedl, B.; Kokta, B. V. Inverse Gas Chromatography Study on Partially Esterified Paper Fiber. *J. Chromatogr. A* **2002**, *969*, 301−311.

(24) Trejo-O'Reilly, J.-A.; Cavaille, J.-Y.; Belgacem, N. M.; Gandini, A. Surface Energy and Wettability of Modified Cellulosic Fibres for Use in Composite Materials. *J. Adhes.* **1998**, *67*, 359−374.

(25) Botaro, V. R.; Gandini, A. Chemical Modification of the Surface of Cellulosic Fibres. 2. Introduction of Alkenyl Moieties via Condensation Reactions Involving Isocyanate Functions. *Cellulose* **1998**, *5*, 65−78.

(26) Felix, J. M.; Gatenholm, P.; Schreiber, H. P. Controlled Interactions in Cellulose−Polymer Composites. 1: Effect on Mechanical Properties. *Polym. Compos.* **1993**, *14*, 449−457.

(27) Matuana, L. M.; Woodhams, R. T.; Balatinecz, J. J.; Park, C. B. Influence of Interfacial Interactions on the Properties of PVC/Cellulosic Fiber Composites. *Polym. Compos.* **1998**, *19*, 446−455.

(28) Matuana, L. M.; Balatinecz, J. J.; Park, C. B.; Woodhams, R. T. Surface characteristics of chemically modified newsprint fibers determined by inverse gas chromatography. *Wood Fiber Sci.* **1999**, *31*, 116−127.

(29) Gamelas, J. A. F.; Pedrosa, J.; Lourenço, A. F.; Ferreira, P. J. Surface Properties of Distinct Nanofibrillated Celluloses Assessed by Inverse Gas Chromatography. *Colloids Surf., A* **2015**, *469*, 36−41.

(30) Kamdem, D. P.; Riedl, B. Inverse Gas Chromatography of Lignocellulosic Fibers Coated with a Thermosetting Polymer: Use of Peak Maximum and Conder and Young Methods. *J. Colloid Interface Sci.* **1992**, *150*, 507−516.

(31) Santos, J. M. R. C. A.; Guthrie, J. T. Analysis of Interactions in Multicomponent Polymeric Systems: The Key-Role of Inverse Gas Chromatography. *Mater. Sci. Eng., R* **2005**, *50*, 79−107.

DOI: 10.1021/acs.langmuir.6b03970
Langmuir XXXX, XXX, XXX−XXX

(32) Mohammadi-Jam, S.; Waters, K. E. Inverse Gas Chromatography Applications: A Review. *Adv. Colloid Interface Sci.* **2014**, *212*, 21−44.
(33) Belgacem, M. N.; Czeremuszkin, G.; Sapieha, S.; Gandini, A. Surface Characterization of Cellulose Fibres by XPS and Inverse Gas Chromatography. *Cellulose* **1995**, *2*, 145−157.
(34) Schultz, J.; Lavielle, L.; Martin, C. The Role of the Interface in Carbon Fibre−Epoxy Composites. *J. Adhes.* **1987**, *23*, 45−60.
(35) Carvalho, M. G.; Santos, J. M. R. C. A.; Martins, A. A.; Figueiredo, M. M. The Effects of Beating, Web Forming and Sizing on the Surface Energy of Eucalyptus Globulus Kraft Fibres Evaluated by Inverse Gas Chromatography. *Cellulose* **2005**, *12*, 371−383.
(36) Saša, B.; Odon, P.; Stane, S.; Julijana, K. Analysis of Surface Properties of Cellulose Ethers and Drug Release from their Matrix Tablets. *Eur. J. Pharm. Sci.* **2006**, *27*, 375−383.
(37) Rani, P. R.; Ramanaiah, S.; Reddy, K. S. Lewis Acid−Base Properties of Cellulose Acetate Butyrate by Inverse Gas Chromatography. *Surf. Interface Anal.* **2011**, *43*, 683−688.
(38) Harding, P. H.; Berg, J. C. The role of adhesion in the mechanical properties of filled polymer composites. *J. Adhes. Sci. Technol.* **1997**, *11*, 471−493.
(39) Marczak, J.; Kargol, M.; Psarski, M.; Celichowski, G. Modification of Epoxy Resin, Silicon and Glass Surfaces with Alkyl- or Fluoroalkylsilanes for Hydrophobic Properties. *Appl. Surf. Sci.* **2016**, *380*, 91−100.
(40) Dorris, G. M.; Gray, D. G. Adsorption of *n*-Alkanes at Zero Surface Coverage on Cellulose Paper and Wood Fibres. *J. Colloid Interface Sci.* **1980**, *77*, 353−362.
(41) Gamelas, J. A. F.; Santos, J. M. R. C. A.; Ferreira, P. J. Surface Energetics of Softwood Kraft Pulps by Inverse Gas Chromatography. In *Characterisation of the Fine Structure and Properties of Papermaking Fibres Using New Technologies*; Ander, P., Bauer, W., Heinemann, S., Kallio, P., Passas, R., Treimanis, A., Eds.; COST Action E54, 2011; Chapter 1, pp 39−49.
(42) Gamelas, J. A. F.; Ferraz, E.; Rocha, F. An Insight into the Surface Properties of Calcined Kaolinitic Clays: The Grinding Effect. *Colloids Surf., A* **2014**, *455*, 49−57.
(43) Gamelas, J. A. F.; Martins, A. G. Surface Properties of Carbonated and Non-Carbonated Hydroxyapatites Obtained after Bone Calcination at Different Temperatures. *Colloids Surf., A* **2015**, *478*, 62−70.
(44) Pedrosa, J.; Gamelas, J. A. F.; Lourenço, A. F.; Ferreira, P. J. Surface Properties of Calcium Carbonate Modified with Silica by Sol−Gel Method. *Colloids Surf., A* **2016**, *497*, 1−7.

DOI: 10.1021/acs.langmuir.6b03970
Langmuir XXXX, XXX, XXX−XXX